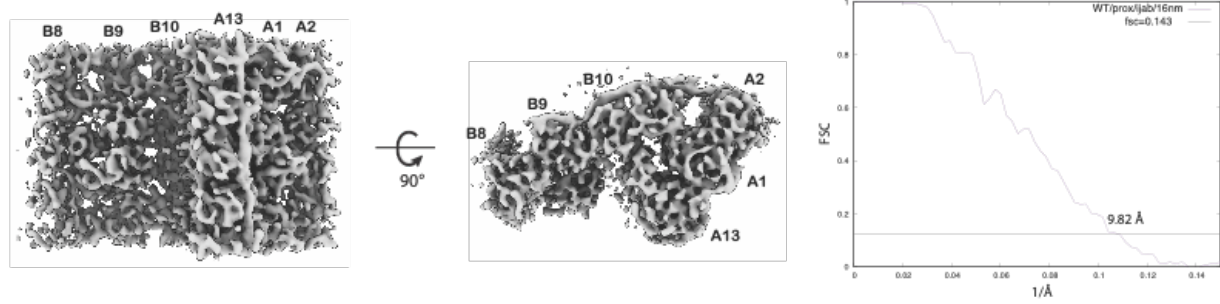
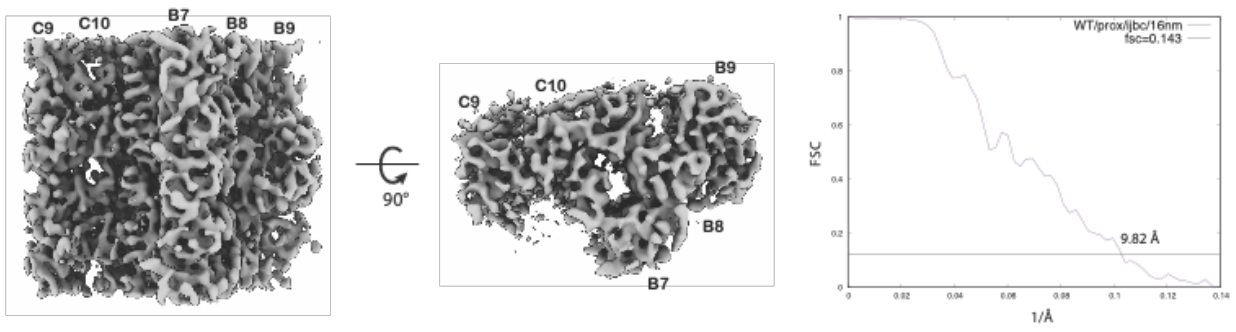


## Figure S1

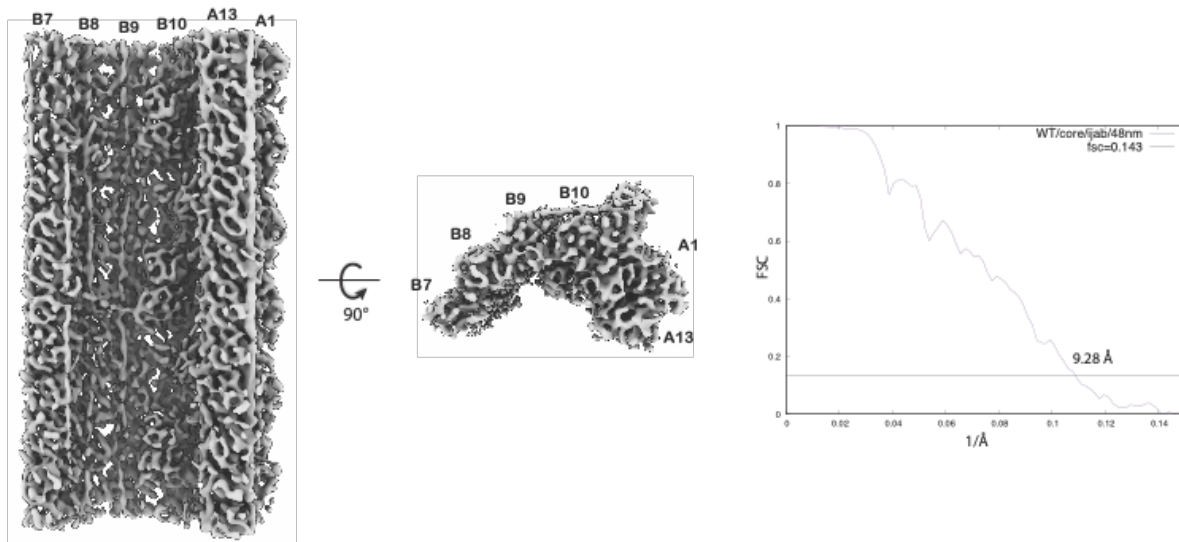
A.



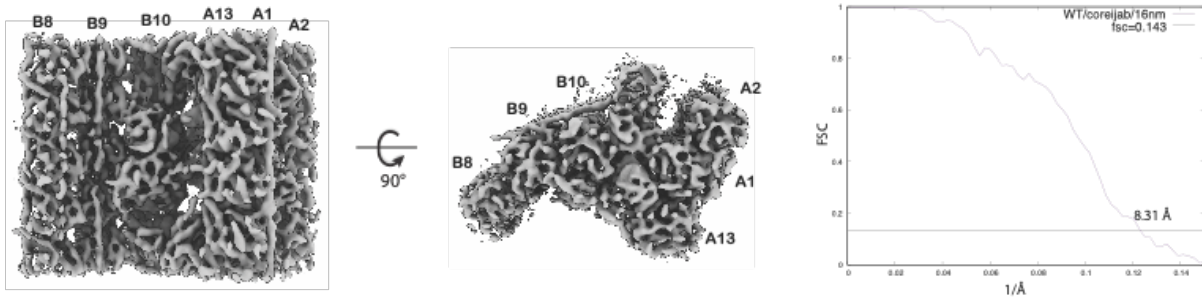
B.



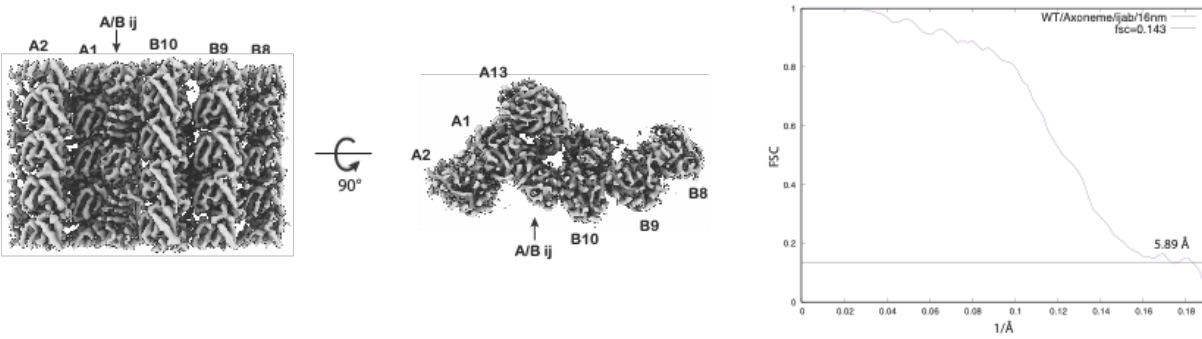
C.



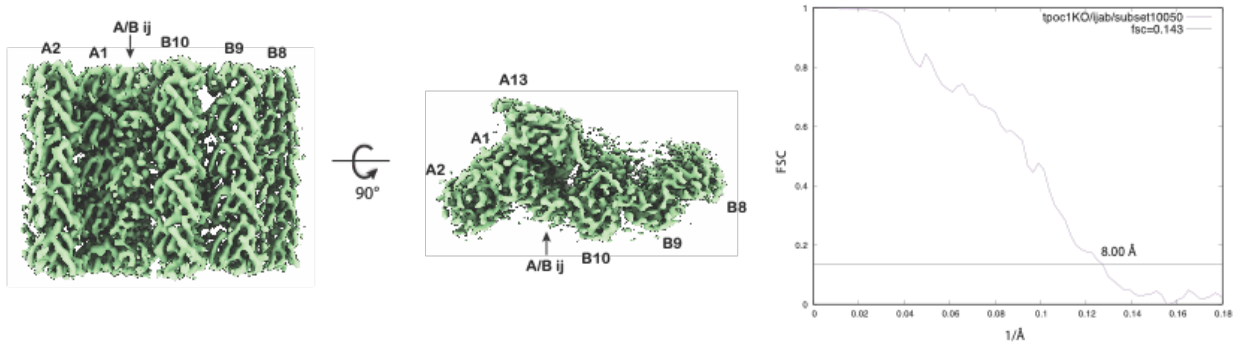
D.



E.



F.



G.

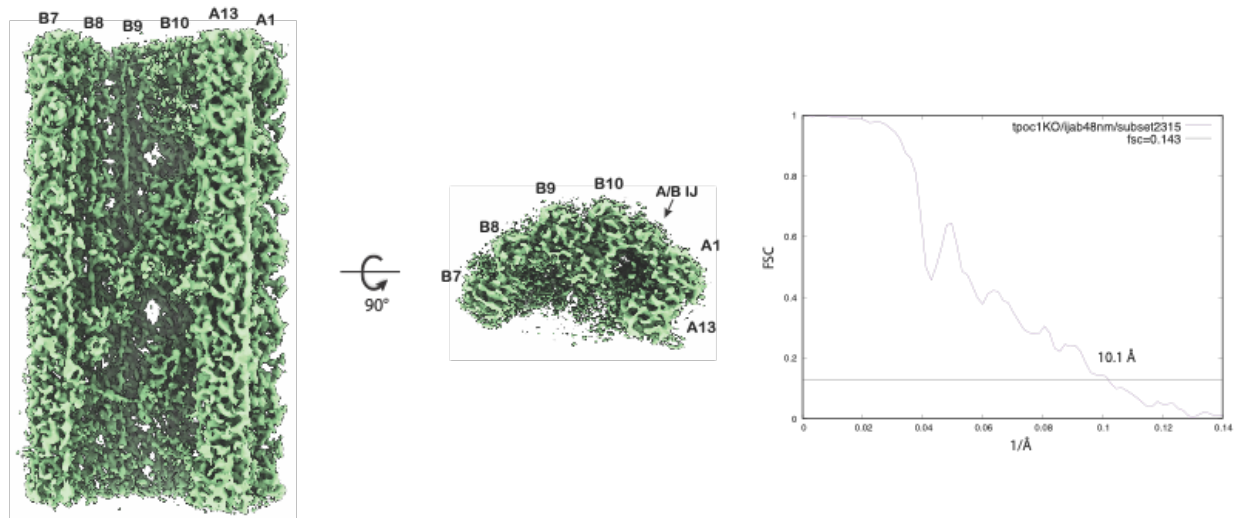


**Figure S1.** Related to Figures 1, 2, 4, 5, S5. Assessing resolution of subtomogram averages by Fourier shell correlation (FSC). The structures and their Fourier shell correlation as a function of resolution ( $1/\text{\AA}$ ) as reported in Table 1. (A) A 16-nm repeat of the A-B inner junction from the proximal region of BB (wild-type). (B) A 16-nm repeat of the B-C inner junction from the proximal region of BB (wild-type). (C) A 48-nm repeat of the A-B inner junction from the central core region of BB (wild-type). (D) A 16-nm repeat of the A-B inner junction from the central core region of BB (wild-type). (E) A 16-nm repeat of the A-B inner junction from the axoneme (wild-type). (F) A 16-nm repeat of the A-B inner junction from a subset (Class 3) of the central core region of *poc1Δ* BB. (G) A 48-nm repeat of the A-B inner junction from a subset (Class 3) of the central core region of *poc1Δ* BB.

Figure S2

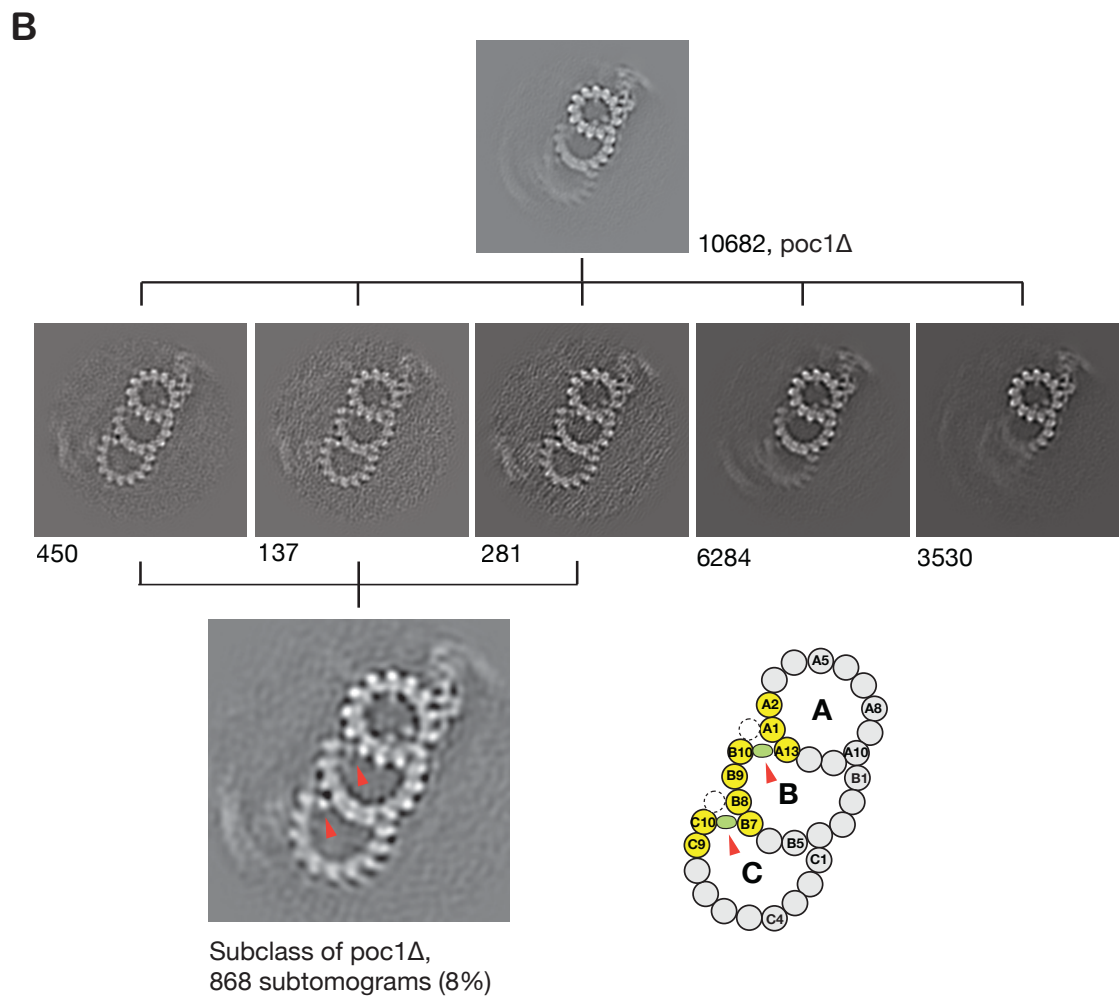
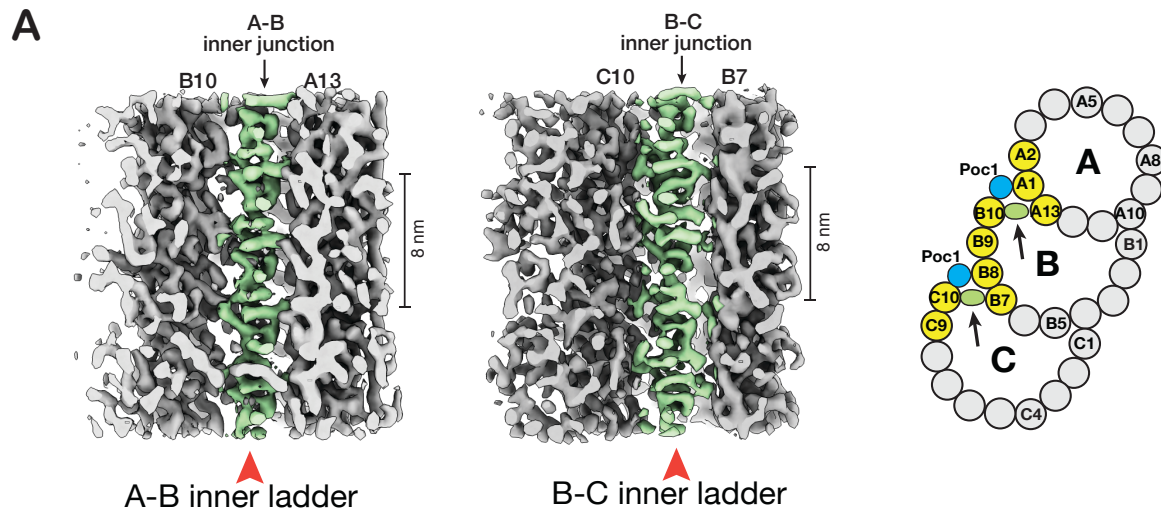
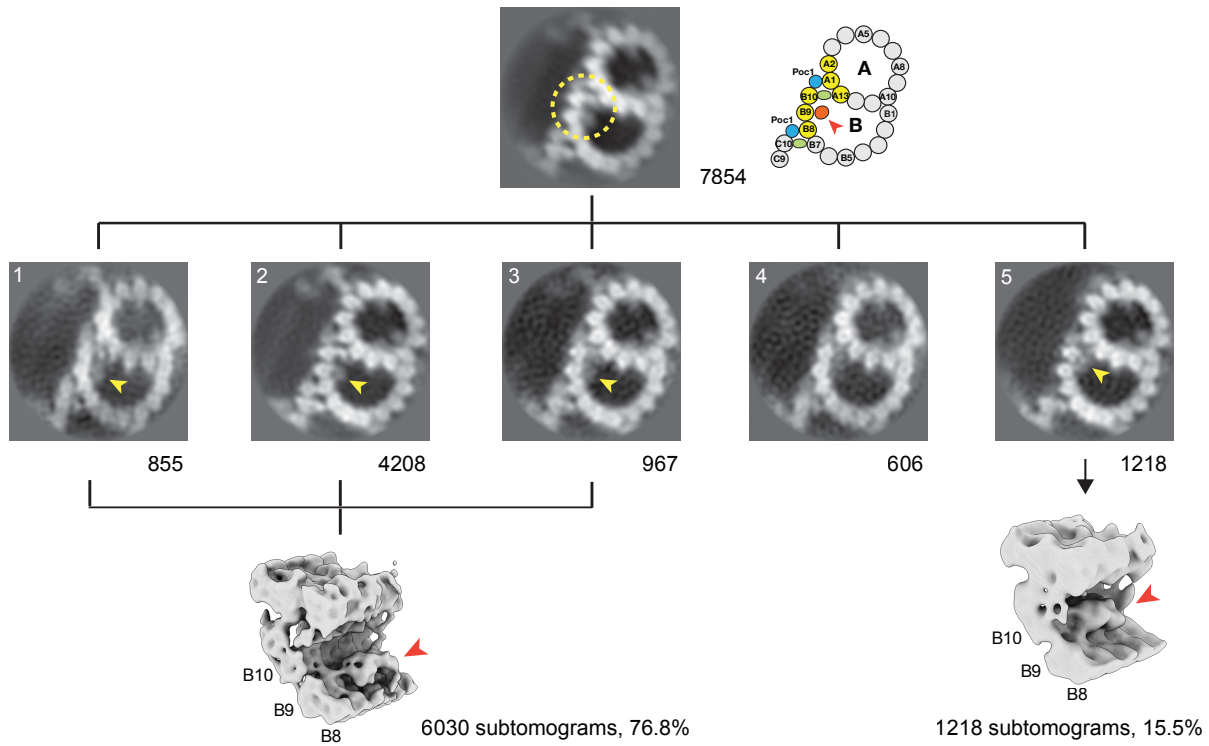


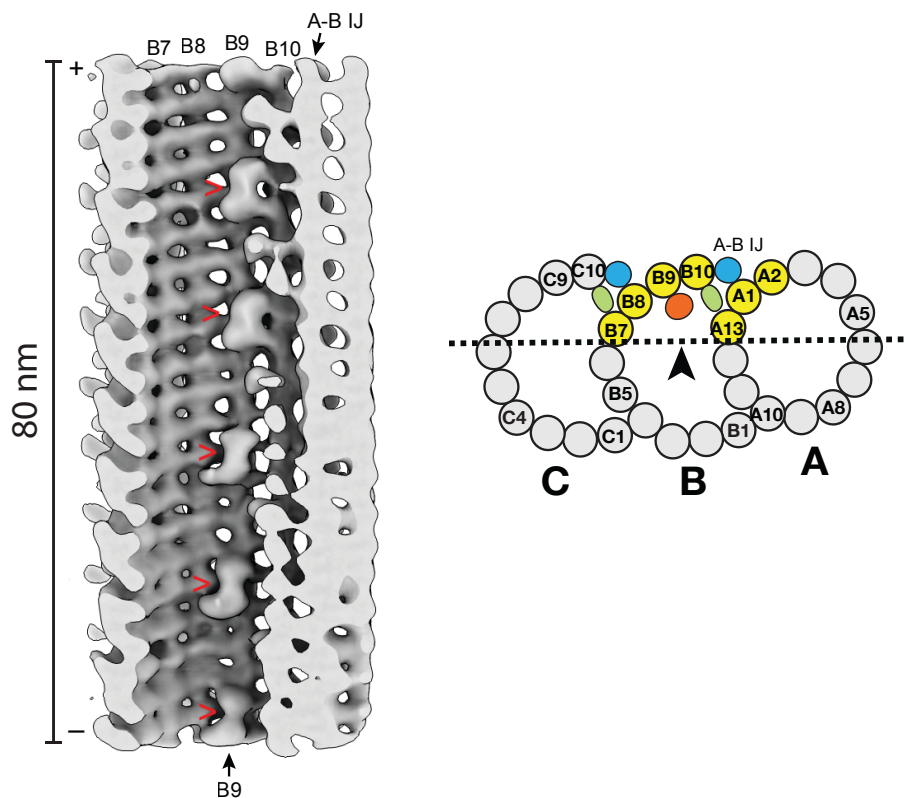
**Figure S2.** *Related to Figure 2.* Two unidentified proteins at the inner junctions in the proximal region. (A) The density maps of the A-B and B-C inner junctions in the proximal region of BB. The two unidentified proteins, namely the A-B inner ladder and B-C inner ladder crosslinking pfs A13-B10 or B7-C10, respectively, are highlighted in green and indicated by red arrowheads. On the right, a schematic diagram shows the location of the above two maps in the TMT. Black arrows indicate the viewing directions. (B) 3D Classification of the subtomograms from the proximal region of *poc1Δ* TMT. A small fraction of the dataset (8%) shows complete TMT, where the two unidentified proteins, the A-B inner ladder and B-C inner ladder indicated by red arrowheads, remain in the inner junctions. The number of subtomograms in each class is shown. The dashed circles in the cartoon indicate the location of Poc1 in the wild-type.

## Figure S3

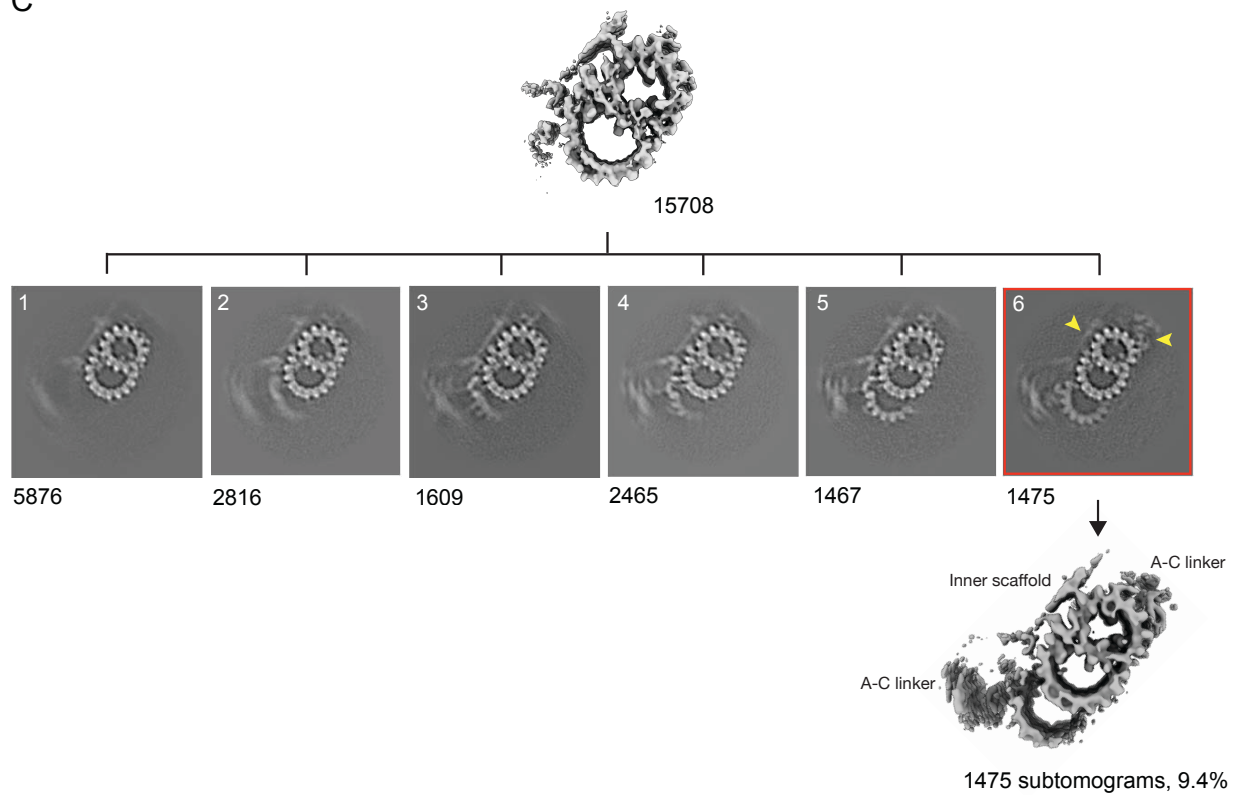
A



B

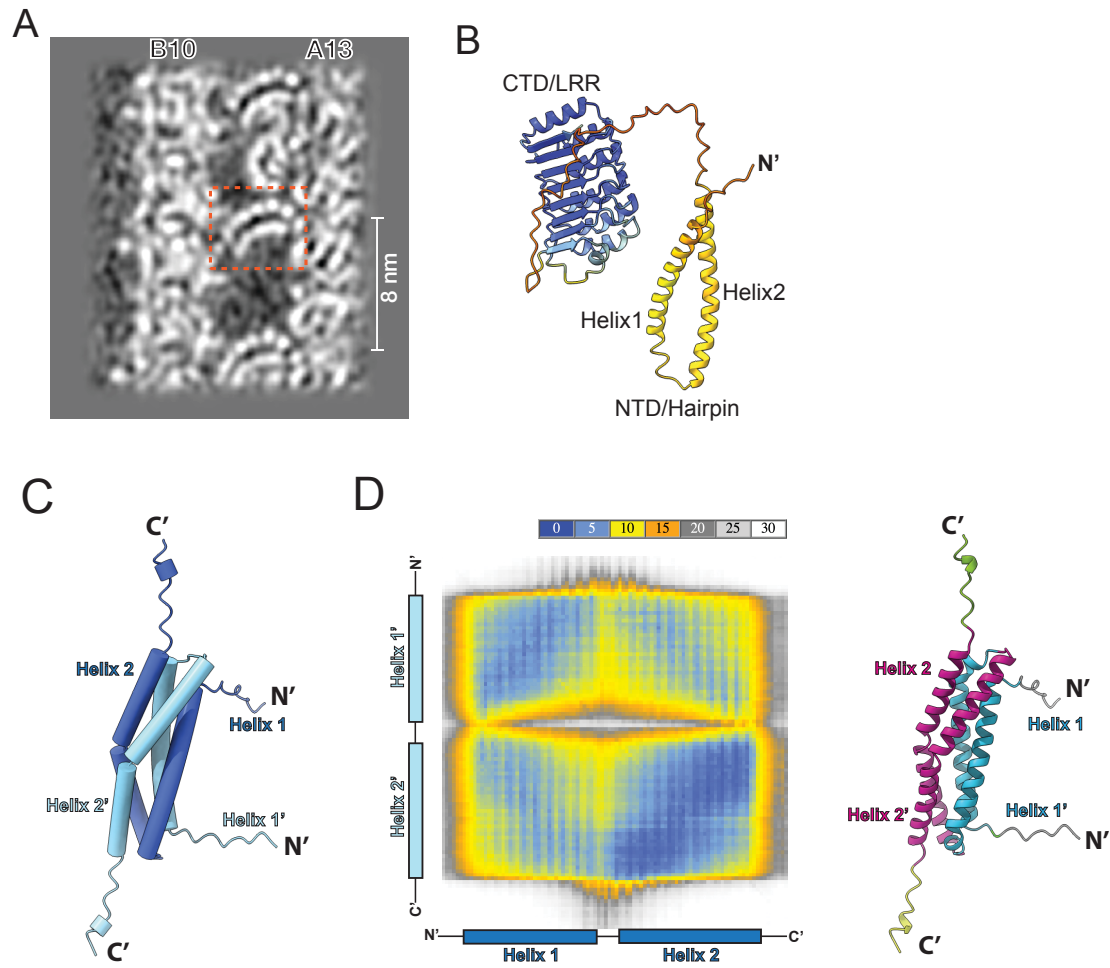


C

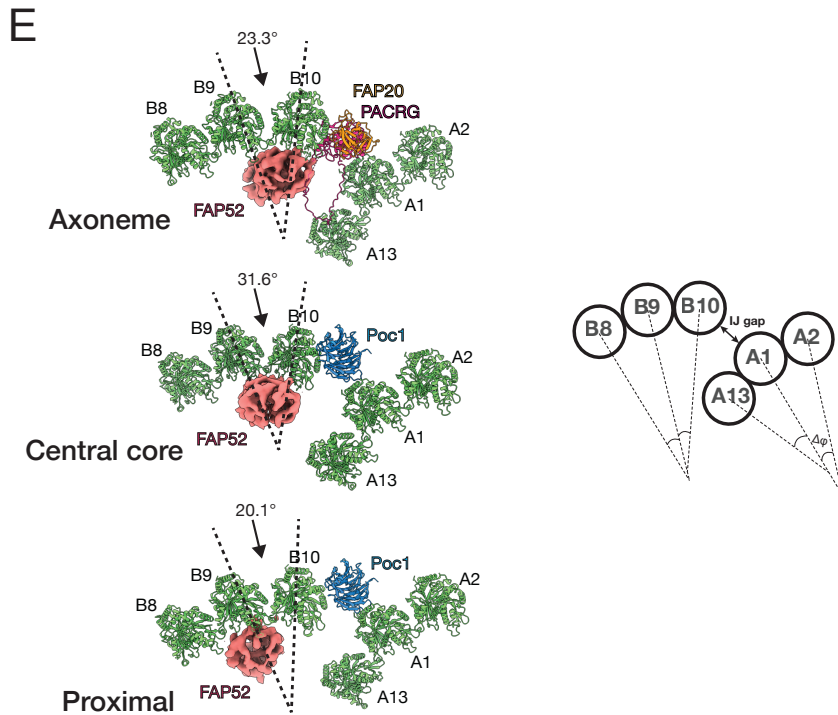


**Figure S3.** *Related to Figure 3.* (A) Focused 3D classification on the subtomograms from the proximal region of the BB. A yellow dashed circle indicates the focused area centered on the inner junction. Yellow or red arrowheads indicate the locations of FAP52 in the class averages. (B) A Longitudinal cross-section of the A-B inner junction showing the FAP52, indicated with red arrowheads, shifts binding from pf B9 to pf 9/10. A schematic illustration of the TMT is on the right. A dashed line and arrow indicate the cross-section and viewing direction of the structure on the left. An orange circle represents FAP52. (C) Focused 3D classification on the subtomograms from the central core region of the BB. The Class 6 is highlighted with a red frame. In this class, the A-C linker and the inner scaffold are indicated by yellow arrowheads. The number of subtomograms in each group is provided.

**Figure S4**



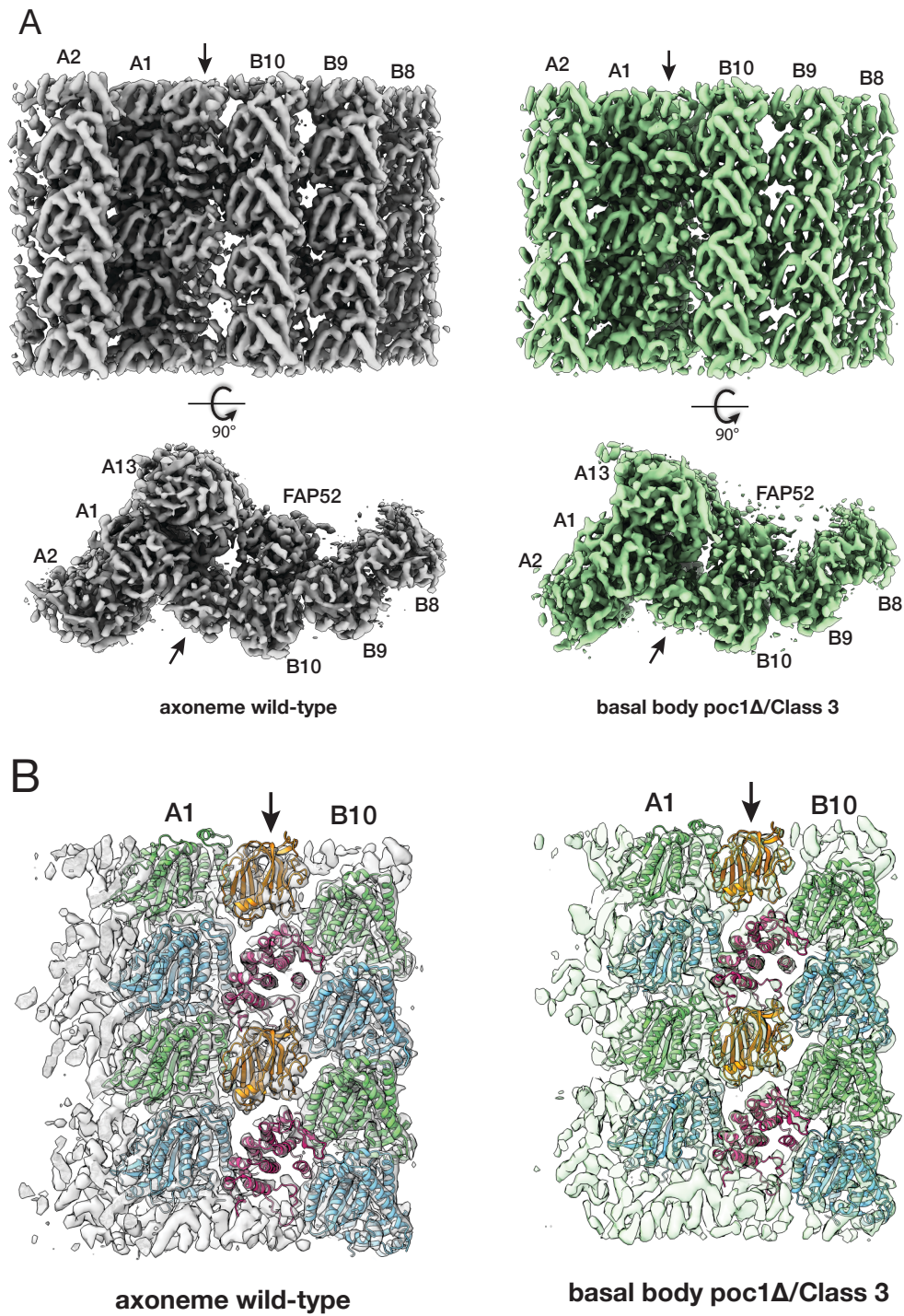




**Figure S4.** *Related to Figure 4.* (A) A cross-section slice of the density map shows an LRR motif highlighted in a red dashed-line square. (B) An AlphaFold2 predicted protein structure (UniProt Q22N53) was identified previously in the BB proteome. The protein is composed of a N-terminal  $\alpha$ -helix hairpin (NTD) and a C-terminal LRR motif (CTD). The structure is colored based on the prediction confidence score (pLDDT: the predicted local distance difference test). The high confidence is in dark blue, while the low confidence is in yellow or orange. (C) An AlphaFold3 predicted 4-helix bundle formed by dimerizing two NTD/hairpins. Two copies of the NTD hairpin form an anti-parallel dimer. One monomer is in dark blue (Helix 1 and Helix 2) and the other monomer is in light blue (Helix 1' and Helix 2'). The dimer forms a right-handed 4-helix bundle. (D) The predicted aligned error (PAE) plot provides inter-domain packing confidence scores. The dark and light blue imply the prediction with high confidence, while the grey and white indicate low confidence in the interaction. On the right, a ChimeraX-adapted color scheme is used where the 4-helix bundle is colored based on the PAE potential interaction score. The two N-terminal helices (Helix 1, Helix 1') are in cyan, and the two C-terminal helices (Helix 2 and Helix 2') are in magenta, indicating that the interaction between Helix 1 and Helix 1' (cyan), Helix 2 and Helix 2' (magenta) are with high confidence. (E) Inter-protofilament angle measurement. Left: the

angles between pfs B9 and B10 are measured at the three regions, showing varying local curvature. The FAP52 and Poc1 or FAP20/PACRG are shown as reference points. Right: a schematic diagram depicts the inter-protofilament angles at the A-B inner junction. More complete measurements are in Table 2.

**Figure S5**



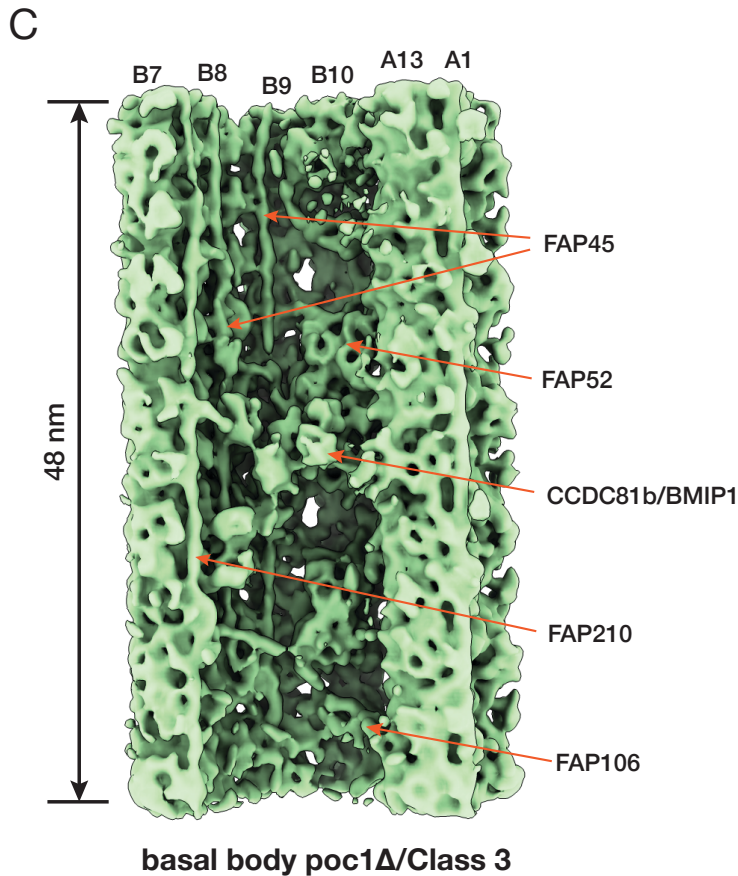


**Figure S5.** *Related to Figure 5.* Comparing the inner junctions between the wild-type axoneme and the Class 3 from the poc1Δ BBs. (A) Comparing the two structures in two orthogonal views, the wild-type axoneme is in grey, and the poc1Δ BB is in green. (B) Fitting the molecular models into the density maps in (A). The  $\alpha/\beta$  tubulins are in light green and blue, FAP20 is in orange, and PACRG is in purple. The arrows indicate the A-B inner junctions. (C) A 48-nm repeat average from a subset of poc1Δ BB (Class 3) shows nearly identical structure to the wild-type axoneme inner junction. This is the same subset as shown in Figure 5E, but here the longitudinal length is extended to 48 nm. For clarity, the map is low-pass filtered to 12 Å.